

The Buncher and the Magnetic Lens for the LINAC Based Low Energy Positron Beams at AIST

Hiroyuki HIGAKI, Koji MICHISHIO¹⁾, Akira ISHIDA²⁾ and Nagayasu OSHIMA¹⁾

*Graduate School of Advanced Science and Engineering, Hiroshima University,
1-3-1 Kagamiyama, Higashi-Hiroshima 739-8530, Japan*

¹⁾*National Institute of Advanced Industrial Science and Technology (AIST),
1-1-1 Umezono, Tsukuba, Ibaraki 305-8568, Japan*

²⁾*Graduate School of Science, The University of Tokyo,
7-3-1 Hongo, Bunkyo, Tokyo 113-0033, Japan*

(Received 15 December 2022 / Accepted 28 February 2023)

A buncher and a magnetic lens were introduced to improve the beam flux density of a pulsed positron beam extracted from the low energy positron accumulator at National Institute of Advanced Industrial Science and Technology (AIST). The buncher made the pulse width $\sim 1/4$ and the magnetic lens reduced the beam cross section $\sim 1/9$, which resulted in about 36 times increase in the beam flux density. Possible applications for electron-positron plasma experiments are also discussed.

© 2023 The Japan Society of Plasma Science and Nuclear Fusion Research

Keywords: low energy positron beam, beam bunching, beam focusing, low energy positron plasma, electron-positron plasma

DOI: 10.1585/pfr.18.1406023

1. Introduction

The low energy positron beams supplied from electron linear accelerators (LINACs) were used more than 40 years in material sciences and atomic physics, which was made possible with the introduction of proper moderators [1]. Since the measurement time can be shorter, the higher intensity positron beam is preferable. In a simple situation, the positron beam intensity may be increased just by increasing the electron current, electron energy or the repetition rate in the LINAC, unless the production target is not damaged. However, in some research activities, it is desirable to have the shorter pulsed low energy positron beams with the higher intensity. For example, if a physical process in concern has a time scale in the order of a few tens of nanoseconds, the pulse width in the order of a nanosecond may be necessary.

One technique to resolve the situation is the so called trap-based low energy positron beam source, which utilizes a radioisotope (RI) and a buffer gas trap to accumulate low energy (≤ 1 eV) positrons. The accumulated positrons are extracted as a pulsed beam from the trap. In the past few decades, those accumulated low energy positrons have been applied for various research fields, i.e., producing antihydrogen atoms and positron systems like positronium (Ps), Ps₂ molecules, Ps⁻, etc. for precision spectroscopy, atomic collision studies, and so on [2]. It is thought that the further bunching and focusing of the pulsed positron beams with the higher intensity (more positrons) will extend the research capabilities.

It seems that there are two possibilities to obtain high intensity beams. The one is to develop the nuclear reactor based low energy positron accumulator, where the multi-cell trap may be introduced to increase the number of positrons further [3]. In principle, a multi-cell trap is also applicable for low energy positrons from an RI and a LINAC. The feasibility depends on the confinement time and the extraction scheme of the multi-cell trap under development. The other possibility is to utilize an electron LINAC, which is also expected to provide higher intensity positron beams compared with RI sources. As mentioned, the use of electron LINAC for the production of low energy positron beams is a standard technique prevailing all over the world. However, the accumulation of LINAC based low energy positrons has not been achieved until recently [4–6]. Here, the timed buncher and the magnetic lens are newly installed for the LINAC based low energy positron accumulator at AIST to improve the intensity of extracted positron pulses.

2. LINAC at AIST

The electron LINAC at AIST accelerates electron bunches supplied by the electron gun shown in Fig. 1 (a) to 40 MeV at 40 Hz with two acceleration tubes (Fig. 1 (b)). The typical pulse width is 2 μ s and the peak current is 100 mA. These accelerated electrons, impinging the water cooled Ta target, create high energy positrons, which go into the biased W moderator (Fig. 1 (c)). The energy of the moderated slow positrons can be controlled with the bias voltage of the W moderator, which is typically less

author's e-mail: hhigaki@hiroshima-u.ac.jp

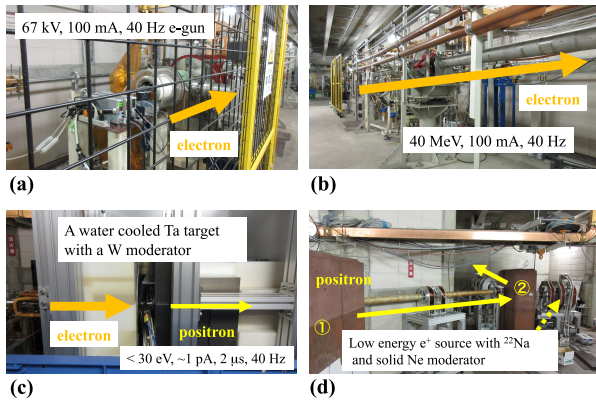


Fig. 1 (a) The electron gun provides 67 keV electron pulses at 40 Hz with the peak intensity of 100 mA. (b) Two RF cavities accelerate the $2\text{ }\mu\text{s}$ electron pulses to 40 MeV. (c) Pair creations at the water cooled Ta target provide high energy positrons, which are moderated at W placed right after the Ta target. (d) The moderated positrons go through two 45 degree corners and guided to the experimental hall behind the concrete wall.

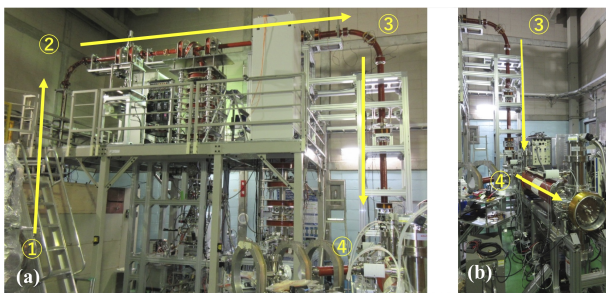


Fig. 2 (a) The positron pulses with the energy less than 30 eV are guided with a magnetic field of about 100 G. There are four 90 degree corners inside the experimental hall before entering the buffer gas trap. (b) The moderated positrons are transported about 20 m long guide field from the moderator to the trap.

than 30 eV, here. The moderated mono-energetic positron pulses are guided through a magnetic field of $\sim 100\text{ G}$ to the experimental hall [7]. The average current of the slow positron pulses is about 1 pA with the pulse width of $2\text{ }\mu\text{s}$. After the moderator, there are two 45 degree corners (Fig. 1 (d)) and four 90 degree corners (Fig. 2) in the positron transfer line to the positron accumulator. The slow positron facility at AIST is unique in that the RI based positron source is also equipped for the same positron transfer line.

3. Low Energy Positron Accumulator

As already mentioned, electron LINACs have been used widely for producing slow positron pulses. Although the accumulation of LINAC based low energy positrons was pursued more than 30 years, it was not realized un-

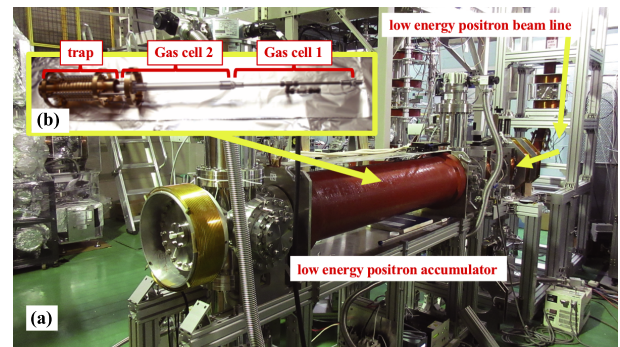


Fig. 3 (a) The buffer gas trap originally used for the RI based positron accumulator was attached to one of the positron transfer lines at the slow positron facility in AIST. (b) The solenoid coil with the length of 1300 mm contains the gas cell 1, 2 and the multi-ring electrode trap.

til recently. In fact, the way to realize the accumulation of a LINAC based low energy positrons has already well established for the accumulation of RI based low energy positrons, i.e., a buffer gas trap. The positron accumulator shown in Fig. 3 (a) in this experiment is the same one used for the accumulation of RI based low energy positrons in previous experiments [8]. Since the intensity of ^{22}Na RI source became lower, the accumulator was transported to AIST to continue experiments. It should be also mentioned that this accumulator is quite similar to the one originally developed by UCSD group [9].

The details of the accumulator were reported before [8]. The solenoid coil with the length of 1300 mm can provide a uniform magnetic field of $\sim 600\text{ G}$ inside the vacuum chamber, which contains two gas cells and the trap shown in Fig. 3 (b). The gas cell 1 and 2 have the inner diameter of 7.6 and 23 mm with the axial length of 400 and 500 mm, respectively. The positron trap has 13 ring electrodes with the inner diameter of 60 mm. The axial length of the trap is 282 mm and one of the ring electrodes is segmented into 4 pieces, so that the rotational electric field can be applied. The minor modification was made to attach the extra gas inlet at the downstream side to introduce CF_4 cooling gas into the trap region. At the base pressure of $\sim 2 \times 10^{-9}$ Torr, N_2 buffer gas and CF_4 cooling gas with the partial pressure of $\sim 2 \times 10^{-6}$ Torr are introduced into the trap. A micro-channel plate (MCP) and a phosphor screen (PS) are installed at the end of the vacuum chamber, where the field strength is about 150 G. With the use of a CCD camera, an image of an extracted positron pulse can be observed after accumulating positrons in the buffer gas trap.

Shown in Fig. 4 (a) is a schematic of the positron trap. The ring electrode named C and S denote the center ring electrode and segmented electrodes, respectively. Also shown in Fig. 4 (b) is an example of the accumulation potential on the axis of symmetry. The axial position $z = 0$

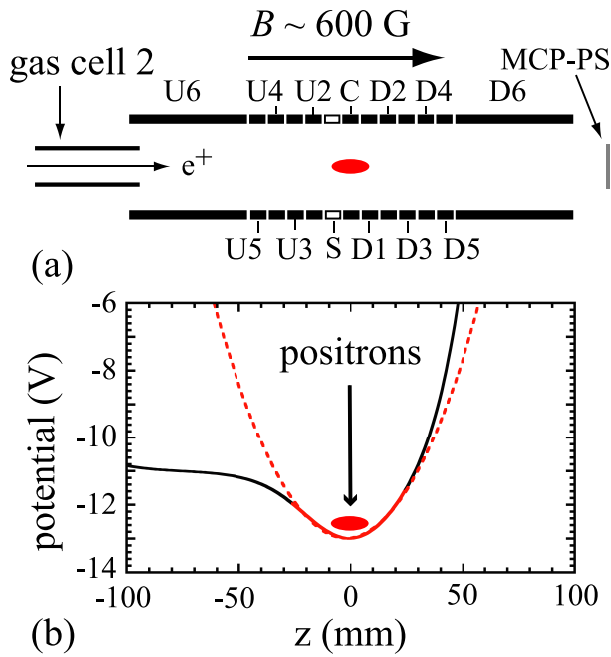


Fig. 4 (a) A schematic of the multi-ring electrodes of the trap, where positrons are accumulated. The ring electrode named C and S denote the center ring electrode and segmented electrodes, respectively. (b) An example of the potential on the axis. The axial position $z = 0$ corresponds to that of the electrode C.

corresponds to that of the electrode C. By injecting 10 eV, $2 \mu\text{s}$ positron pulses at 40 Hz, 5×10^5 positrons were accumulated in 4 s with a rotational electric field. The accumulated positrons can be extracted with a much shorter pulse width of ~ 9 ns. And the Gaussian beam profile observed at the position of the PS has a full width at the half maximum (FWHM) of ~ 1.8 mm [5].

Regarding the accumulated positron number N , the simple fitting curve,

$$N = \alpha\tau[1 - \exp(-t/\tau)], \quad (1)$$

leads to the accumulation rate $\alpha = 1.7 \times 10^5 \text{ s}^{-1}$ and the confinement time $\tau = 2.8$ s. And the trapping efficiency was about 4%. Unfortunately, these values were less compared with those of RI based positron accumulators. This is probably due to a wide axial energy spread of the incoming positron pulses. Shown in Fig. 5 are the output signals of a scintillator placed at the end of the accumulator where positrons annihilate by hitting the MCP at the end of the beam line. The retarding potential is applied to the gas cell 1 at the field strength of ~ 600 G for various incoming energies of the positron pulses. It is clearly seen that the axial energy distributions inside the accumulator are almost flat for the measured positron energy of 7, 10, 15 and 20 eV. In contrast, the previous RI based positron source with the solid Ne moderator had the axial energy spread less than 4 eV for the injection energy of 50 eV [8]. Since the electronic excitation of N_2 molecule is the main

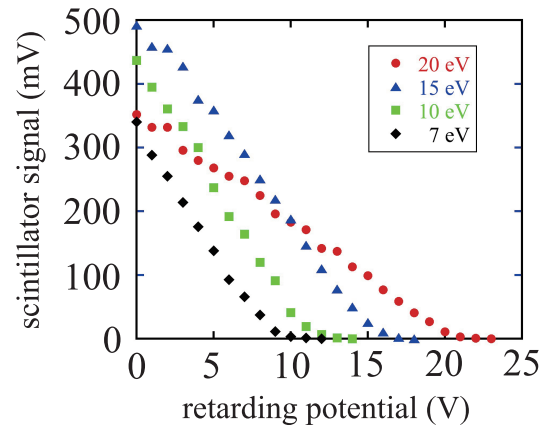


Fig. 5 The scintillator signals observed as a function of the retarding potential applied at the gas cell 1 at $B \sim 600$ G. It is seen that the axial energy distributions are almost flat for all injection energies of positrons.

energy loss process for trapping positrons, which has the large cross section for the specific energy around 9 eV, it is thought that the observed large energy spread deteriorates the trapping efficiency.

There are two possible reasons for this large axial energy spread. One is the magnetic mirror effect at the entrance of the accumulator, where the field changes from 100 to 600 G (In case of the previous setup with RI source, the field changes from 360 to 900 G). The other possibility is the gradient B drift due to the 6 corners in the positron transport line. However, it is thought that the effect of the gradient B drift is not so serious at the lower energy. Even if the magnetic mirror effect is the reason for the axial energy spread, the field strength at the accumulator cannot be reduced, because the incoming positron beam has to go through the gas cell 1 with the I.D. of 7.6 mm.

A possible solution to improve the trapping efficiency is to use a re-moderator inside the uniform magnetic field of the positron accumulator. One of the candidates for a re-moderator is a silicon carbide (SiC), which was reported to have the re-emission efficiency of $\sim 60\%$ [10]. Then, depending on the operation scheme, it is not necessary to use N_2 buffer gas [11].

4. The Buncher and the Magnetic Lens

Shown in Fig. 6 are a picture and a schematic of the buncher and magnetic lens newly installed to improve the intensity of pulsed positron beams at AIST. The cylindrical buncher electrode has the inner diameter of 8 mm and the axial length of 120 mm, which is housed in a continuous uniform magnetic field ~ 230 G. After the buncher, there is the differential pumping stage which is composed of the cylindrical pipe with the inner diameter of 8 mm and the axial length of 100 mm. Then, the electrostatic acceleration unit composed of two parallel meshes accelerates

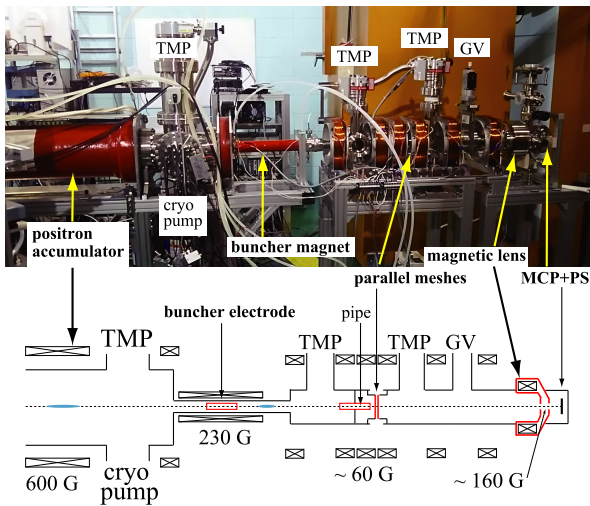


Fig. 6 The buncher and the magnetic lens were newly installed for the low energy positron accumulator at AIST to improve the intensity of extracted positron beams. The MCP and PS are also attached at the end of the beam line to observe the profiles of the extracted positron beams.

positrons to 5 keV. Finally, the accelerated positrons go through the magnetic lens [12, 13] and focused on the MCP and PS. A plastic scintillator is also placed at the end of the beam line to observe the annihilations of positrons at the MCP.

Depending on the research purposes, it is useful to have the higher intensity positron pulses. Ideally, it is better if the space volume of the bunched beam can be reduced while keeping the beam energy constant. However, it is not possible to reduce the phase space volume without a certain cooling mechanism (Liouville’s theorem). This means if the volume in real space is reduced, the volume in velocity space increases, thus it is inevitable to heat up the bunched beam during the compression in the real space. So, if the experimental purpose permits, the following bunching techniques can be applied. Traditional techniques for bunching a low energy positron pulses are so called harmonic buncher and timed potential buncher [14, 15]. A harmonic buncher uses the harmonic potential, which is effective when the positrons extend over some electrodes. In that sense, the multi-ring structure employed in the positron accumulator is suitable for applying the harmonic bunching potential under the condition that a large number of trapped positrons fill over the axial space of the trap. Unfortunately, 5×10^5 positrons are localized at the bottom of the potential near the segmented electrodes and the harmonic bunching is not suitable at the moment. Therefore, a timed potential buncher is employed here.

Basically, the buncher electrode applies an electric potential to the tail of a pulsed beam. In Fig. 7, the concept of a timed buncher is depicted and the inset shows the electric pulse applied to the buncher electrode. At the beginning (i), an extracted positron pulse is contained inside the

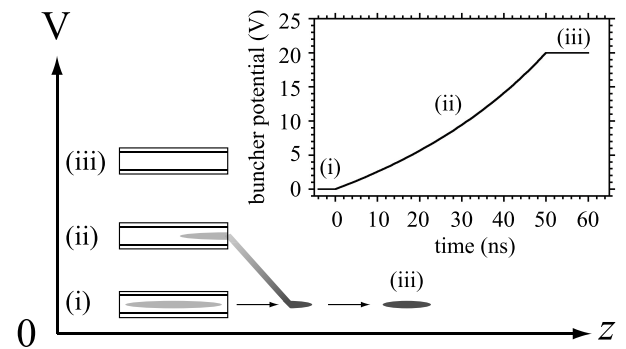


Fig. 7 The concept of a timed buncher. (i) A positron pulse is inside the grounded buncher electrode. (ii) The buncher potential increases so that the remaining part of the pulse has the higher energy. (iii) At the focal point, the shorter pulse results with the higher intensity. The inset shows the electric pulse applied to the buncher electrode.

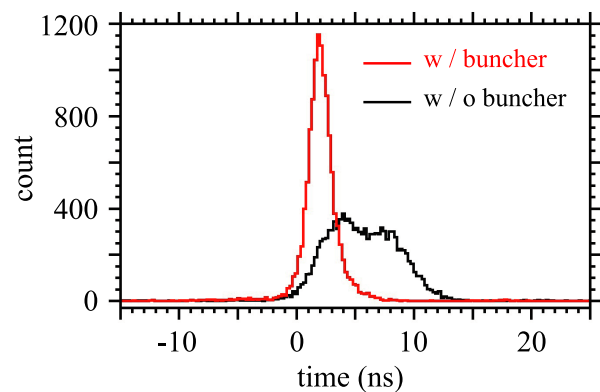


Fig. 8 Pulse widths of the extracted positrons are measured with and without a buncher pulse. The Gaussian fitting of the observed pulses results in 2.2 ns and 7.6 ns, respectively. The pulse is compressed axially 1/4 of the original pulse of 9 ns.

grounded cylindrical buncher. As the pulse go through the buncher (ii), the buncher potential increases monotonically so that the latter part of the pulse has the higher energy. At the focal point (iii), the beam can be compressed axially at the expense of the beam energy spread.

Figure 8 shows the pulse widths of the extracted positron pulses measured with the scintillator. The solid red line is the signal obtained with the buncher pulse and the solid black line is the one without a buncher pulse. The Gaussian fitting of the observed pulses results in FWHM of 2.2 ns and 7.6 ns, respectively. So, the positron pulse is axially compressed about 1/4 of the original pulse (9 ns) without the bunching system [5].

In the transverse plane, perpendicular to the beam axis, the beam can be focused radially with the use of the magnetic lens, which produces the local axial magnetic field over ~ 30 mm along the beam axis. In Fig. 9, the calculated magnetic field on the axis at the position of

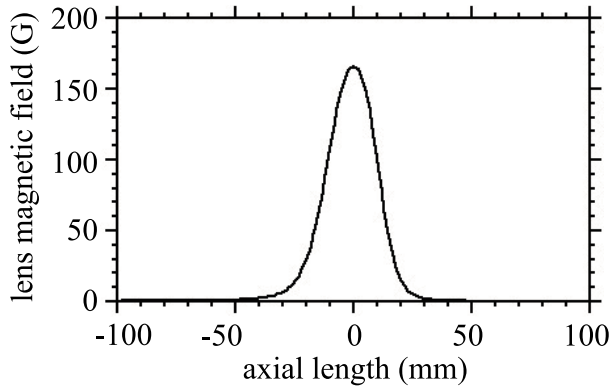


Fig. 9 The calculated magnetic field on the axis produced by the magnetic lens with the coil current of 1.00 A. It is seen that the magnetic field extends over ~ 30 mm in FWHM.

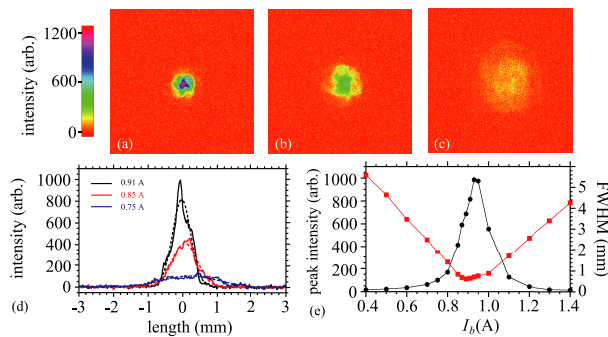


Fig. 10 Images of the extracted positron pulses with the magnetic lens for (a) $I_b = 0.91$ A, (b) $I_b = 0.85$ A, (c) $I_b = 0.75$ A. (d) The cross sections of the images in (a), (b) and (c). (e) The peak intensity (solid circle) and profile width (red square) on PS are plotted as functions of I_b . The minimum FWHM of ~ 0.6 mm ($I_b = 0.89$ A) is $1/3$ of the one (1.8 mm) without the magnetic lens.

the magnetic lens is plotted as an example for the coil current $I_b = 1.00$ A, where the maximum field is about 167 G. The focused beam size was estimated with the paraxial-ray equation in cylindrical coordinates. The similar focusing system was applied for the slow positron beam line at AIST (without the accumulation trap), which resulted in the beam size of ~ 90 μm after a re-moderator [12] and also for the production of Ps^- beam with the smaller diameter to improve the interaction with a crossing laser [13].

Figures 10(a), (b), and (c) show the example images of the positron pulses observed with the CCD camera for three different I_b of 0.91, 0.85, and 0.75 A. In fact, meshes for acceleration can be observed in (a) and (b), and the images are somewhat deformed from a circular profile. It is also confirmed in Fig. 10(d), where the cross sections of the images in (a), (b), and (c) are plotted. Although the beam profiles (solid lines) are slightly deviated from Gaussian fittings (dashed lines), the peak and FWHM of the Gaussian profiles are plotted as functions of I_b in Fig. 10(e), where solid circles and red squares de-

note the peak intensity and FWHM, respectively. The minimum FWHM of ~ 0.6 mm at $I_b = 0.89$ A is $\sim 1/3$ of the one (1.8 mm) before installing the magnetic lens. Therefore, the beam flux density becomes about 36 times higher by introducing the new focusing elements, i.e., the timed buncher and the magnetic focusing lens.

5. Electron - Positron Plasma Experiments

One of possible applications of the LINAC based low energy positron accumulator is to perform the electron-positron (e-p) plasma experiments where a higher intensity shorter positron pulse is preferable. A possible procedure to prepare an e-p plasma in a trap with a closed magnetic field configuration may be as follows. At first, 10^9 electrons are confined in the trap, while positrons are accumulated in a different accumulator. When 10^9 positrons are ready, a pulsed positron beam is injected into the electron plasma by applying a proper guide field. Therefore, the disturbances due to the guide field for positrons on the existing electron plasma can be minimized and the catching efficiency of positrons may be improved with a higher intensity shorter positron pulse. The latter is also true for open magnetic field configurations like a compact magnetic mirror and a uniform magnetic field.

So far, theoretical research activities on e-p plasmas have been conducted intensively, including simulations in some cases, which are listed in Refs. [16] and [17]. Although various interesting phenomena are expected, there is almost no experimental verification. This is partly because the simultaneous confinement of charged particles with different signs of charges is difficult in laboratories. However, even if the confinement time of e-p plasmas is not so long, the confinement can be meaningful when the specific phenomena in concern have a short time scale compared with the confinement time. For example, the plasma oscillation in the order of MHz can be studied if the confinement time is longer than 10 ms.

As the methods of accumulating low energy positrons in a Penning-Malmberg trap become established, some e-p plasma experiments are proposed, which include various magnetic configurations. A simple stellarator (helical magnetic field) with two ring coils [18] and a compact levitated dipole field with a superconducting magnet [19] are planned with the use of a multi-cell trap, which accumulates $10^{10} - 10^{11}$ positrons [3]. A good old magnetic mirror field [20] may be used finally for the confinement of high energy e-p plasmas, whose electrons and positrons are from the pair creations with high intensity lasers [21]. A compact magnetic mirror can be also used for low energy e-p plasmas [22], whose 10^8 positrons can be supplied from a standard positron accumulator. And a nested Malmberg trap in a uniform magnetic field may be the simplest setup for e-p plasma experiments with 10^8 electrons and positrons, respectively [23].

Since the observed physical phenomena depend on the magnetic configuration, unique experimental results are expected for each configuration. For example, the effect of the co-streaming and counter streaming in e-p plasmas can be studied with a stellarator. A dipole magnet is suitable for studying the self-organization of e-p plasmas in a magnetosphere. High energy e-p plasmas in a strong magnetic mirror is unique in that plasma parameters (the density and temperature) are totally different from the other experiments, which may be observed in neutron stars in the universe. Probably, a uniform magnetic field may give a chance to study the vortex interactions between positive and negative vorticities. So, each magnetic configuration has its own uniqueness and they are complementary to each other. Most of these experiments will be made possible with the use of a superconducting magnet for accumulating a large number of positrons ($\geq 10^9$) from the LINAC based low energy positrons.

6. Summary

The timed potential buncher and the magnetic lens system were applied successfully for the low energy positron accumulator at AIST. The original pulse width of 9 ns became 2.2 ns and the original Gaussian beam profile with the FWHM of 1.8 mm was focused to that of 0.6 mm. In total, the beam flux density becomes ~ 36 times higher with the new set up. Although the number of positrons may not be enough for some specific applications, it will be improved by employing a re-moderator inside the accumulator.

There are proposals for electron-positron plasma experiments with various magnetic field configurations, like a stellarator, a magnetic dipole, a magnetic mirror, and a uniform magnetic field, which are complementary to each other. With the use of a (nested) Malmberg trap in a uniform magnetic field (~ 3 T), 10^9 to 10^{10} positrons can be used to investigate electron-positron plasmas experimentally.

This work was partly supported by JSPS KAKENHI Grant, No. 22H04936, 24340142, JP19H01923, and JP17H02820.

- [1] P.J. Schultz and K.G. Lynn, *Rev. Mod. Phys.* **60**, 701 (1988).
- [2] J.R. Danielson, D.H.E. Dubin, R.G. Greaves and C.M. Surko, *Rev. Mod. Phys.* **87**, 247 (2015).
- [3] N.C. Hurst, J.R. Danielson, C.J. Baker and C.M. Surko, *Phys. Plasmas* **26**, 013513 (2019).
- [4] S. Niang, M. Charlton, J.J. Choi *et al.*, *Acta Phys. Pol. A* **130**, 164 (2020).
- [5] H. Higaki, K. Michishio, K. Hashidate, A. Ishida and N. Oshima, *Appl. Phys. Express* **13**, 066003 (2020).
- [6] P. Blumer, M. Charlton, M. Chung *et al.*, *Nucl. Instrum. Methods Phys. Res. A* **1040**, 167263 (2022).
- [7] B.E. O'Rourke, N. Oshima, A. Kinomura and R. Suzuki, *Jpn. J. Appl. Phys. Conf. Proc.* **2**, 011304 (2014).
- [8] H. Higaki, C. Kaga, K. Nagayasu *et al.*, *AIP Conf. Proc.* **1668**, 040005 (2015).
- [9] T.J. Murphy and C.M. Surko, *Phys. Rev. A* **46**, 5696 (1992).
- [10] R. Suzuki, T. Ohdaira, A. Uedono *et al.*, *Jpn. J. Appl. Phys.* **73**, Pt.1, 4636 (1998).
- [11] K. Michishio, H. Higaki, A. Ishida and N. Oshima, *New J. Phys.* **24**, 123039 (2022).
- [12] N. Oshima, R. Suzuki, T. Ohdaira *et al.*, *J. Appl. Phys.* **103**, 094916 (2008).
- [13] K. Michishio, L. Chiari, F. Tanaka, N. Oshima and Y. Nagashima, *Rev. Sci. Instrum.* **90**, 023305 (2019).
- [14] A.P. Jr. Mills, *Appl. Phys.* **22**, 273 (1980).
- [15] R.G. Greaves and J. Moxom, *AIP Conf. Proc.* **692**, 140 (2003).
- [16] E.V. Stenson, J. Horn-Stanja, M.R. Stoneking and T. Sunn Pedersen, *J. Plasma Phys.* **83**, 595830106 (2017).
- [17] M.R. Stoneking, T. Sunn Pedersen, P. Helander *et al.*, *J. Plasma Phys.* **86**, 155860601 (2020).
- [18] T. Sunn Pedersen, J.R. Danielson, C. Hungenschmidt *et al.*, *New J. Phys.* **14**, 035010 (2012).
- [19] H. Saitoh, J. Stanja, E.V. Stenson *et al.*, *New J. Phys.* **17**, 103038 (2015).
- [20] V. Tsytovich and C.B. Wharton, *Comments Plasma Phys. Control. Fusion* **4**, 91 (1978).
- [21] J. von der Linden, G. Fiksel, J. Peebles *et al.*, *Phys. Plasmas* **28**, 092508 (2021).
- [22] H. Higaki, C. Kaga, K. Fukushima *et al.*, *New J. Phys.* **19**, 023016 (2017).
- [23] H. Higaki, K. Ito and H. Okamoto, *Jpn. J. Appl. Phys.* **58**, 080912 (2019).